

# RSC Advances



This is an *Accepted Manuscript*, which has been through the Royal Society of Chemistry peer review process and has been accepted for publication.

*Accepted Manuscripts* are published online shortly after acceptance, before technical editing, formatting and proof reading. Using this free service, authors can make their results available to the community, in citable form, before we publish the edited article. This *Accepted Manuscript* will be replaced by the edited, formatted and paginated article as soon as this is available.

You can find more information about *Accepted Manuscripts* in the [Information for Authors](#).

Please note that technical editing may introduce minor changes to the text and/or graphics, which may alter content. The journal's standard [Terms & Conditions](#) and the [Ethical guidelines](#) still apply. In no event shall the Royal Society of Chemistry be held responsible for any errors or omissions in this *Accepted Manuscript* or any consequences arising from the use of any information it contains.

## Photocatalytic dye degradation properties of wafer level GaN nanowires by catalytic and self-catalytic approach using chemical vapor deposition

V. Purushothaman,<sup>1</sup> S. Prabhu,<sup>2</sup> K. Jothivenkatachalam,<sup>2</sup> S. Parthiban,<sup>3</sup> J. Y. Kwon<sup>3</sup> and

K. Jeganathan<sup>1,\*</sup>

1. Centre for Nanoscience and Nanotechnology, School of Physics, Bharathidasan University, Tiruchirappalli, 620024, India.
2. Department of Chemistry, Anna University, Tiruchirappalli-620024, India.
3. School of Integrated Technology, Yonsei University, Songdo-dong, Incheon, 406-840, Republic of Korea

Corresponding author Email – [kjeganathan@yahoo.com](mailto:kjeganathan@yahoo.com), [jagan@physics.bdu.ac.in](mailto:jagan@physics.bdu.ac.in)

### Abstract:

We report the photocatalytic dye degradation properties of self-assembled Gallium Nitride (GaN) nanowires grown using chemical vapor deposition. GaN nanowires have been fabricated using Ni and Au as the catalyst besides the self-catalytic approach. The defect engineered multiband GaN nanowires were subjected to the photocatalytic decay of Methylene Blue (MB), a common dye in the dyeing industry under UV and visible light. Ni-catalyst assisted GaN nanowires possess the maximum degradation of 93% under UV irradiation as correlated with the strong UV band edge emission at 3.42 eV. Interestingly, self-catalytic GaN nanowires shows high photocatalytic activity of 89% under visible irradiation than the catalyst assisted nanowires owing to the presence of radiative surface defects in visible region as evidenced by the photoluminescence studies. The nanowires exhibit enhanced photocatalytic decay as compared to epitaxial layer due to high surface area

and active sites of one-dimensional nanostructures. Detailed analysis further demonstrates the stable photocatalytic activity of the GaN NWs for several cycles against photocorrosion. This work establishes the use of wafer level GaN NWs as a viable photocatalyst for visible light driven decay of organic pollutants.

### **Introduction:**

Models of photosynthesis mimetic systems, or artificial photosynthesis systems, including photoelectrochemical water splitting,<sup>1</sup> photocatalysis<sup>2</sup> and photovoltaic cells,<sup>3</sup> have attracted significant amount of attention because of the abundance of solar resource available, and minimum carbon footprint generated by these systems. Waste water emissions from the textile industry contain large amounts of azo dyes, which are considered a major threat to the surrounding ecosystem due to their non-biodegradability, toxicity, and potential carcinogenicity. Environmental concerns and the need to meet stringent international standards for waste water safety have encouraged the development of novel, efficient, and low-cost processes for purifying textile aqueous effluents. Azo dye removal by photoinduced decomposition of pollutants using photocatalysts has been widely researched.<sup>4</sup> Semiconductor photocatalysts, importantly metal oxides such as TiO<sub>2</sub>, ZnO, Fe<sub>2</sub>O<sub>3</sub>, WO<sub>3</sub>, etc., has received tremendous attention as photocatalysts because these powders can be easily prepared using simple methods.<sup>5,6,7,8,9</sup> However, these photocatalyst nanopowders are generally suspended in water, which limits their practical use because of the difficulty in collecting and recycling photocatalyst powders from a suspension. In order to solve this mobilization problem, immobilized photocatalyst has been suggested by making a photocatalytic thin film or nanostructures strongly attached to a substrate.<sup>4,10,11,12,13</sup> In particular, high density one-dimensional nanostructures are good candidate for photocatalytic applications because photocatalytic activity generally increases with the surface area. Many

industrial processes require photocatalysts that work under harsh conditions such as high chemical environment with low or high pH. Accordingly, it is very important to synthesize a substrate-supported nanostructured photocatalyst that is chemically stable under harsh conditions.

Gallium Nitride (GaN) is one of the most promising semiconducting materials with a direct band gap of 3.4 eV. Although the wide band gap is a drawback for photocatalytic decay under sunlight, GaN has considerably high flat-band potential (approximately equal to conduction band edge for n-type conductors of -1.5 eV), which is advantageous because the photogenerated electrons in the conduction band must have high reduction potential. Furthermore, it has been reported that GaN has an excellent chemical stability in acid or base solutions when compared with the well-known photocatalysts such as TiO<sub>2</sub> and ZnO, which makes it very useful in several industrial processes where pollutant degradation under extreme pH conditions is required. In addition GaN is also expected to enable continuous photocatalytic activity and high numbers of recyclability without degradation.

In the recent past, semiconductor nanostructures such as nanowires (NWs), nanorods and nanotubes have received a great deal of attention for understanding new structures and utilizing them as a building block for future nanoscale devices.<sup>14</sup> Semiconductor NWs have the potential to be used in the field of electronics,<sup>15</sup> optoelectronics,<sup>16</sup> photocatalyst<sup>17</sup> and sensors<sup>18</sup> because of their outstanding electrical, optical, thermal and mechanical properties caused by their size and surface effects. Here, we have investigated the photodegradation of Methylene blue (MB) under UV and visible light using GaN nanowires grown under various conditions. The higher photocatalytic decay of self-catalyst assisted GaN NWs under visible light is ascribed to the defect induced multi band energy levels in the visible region as evidenced by the optical transitions in PL spectrum.

**Experimental Methods:**

A detailed growth process for both the catalytic and self-catalytic approach has already been published elsewhere.<sup>19,20,21</sup> In short GaN NWs were synthesized by the direct reaction of metal Ga and ammonia (NH<sub>3</sub>) in the horizontal CVD reactor. Metal Ga of 0.1 gm (ALFA ACEAR - 99.999%) is taken in a quartz crucible and placed in the alumina boat. A piece of Si (111) (1 x 1 cm<sup>2</sup>) substrate is RCA cleaned and placed on the downstream to the metal Ga. The temperature is kept (@ 900°C) constant for all samples. For catalyst assisted growth, 5 nm thick metal layers (Au and Ni) was deposited by e-beam evaporation method prior to loading into the CVD reactor. N<sub>2</sub> and NH<sub>3</sub> (99.999%) flow of 500 and 200 SCCM (standard cubic centimetre), respectively is used as carrier and reactant gases. For self-catalytic GaN NWs, initially N<sub>2</sub> is flown for 2 min to transport Ga vapours to deposit the Ga droplet layer on the Si substrate that acts as the catalyst for the subsequent growth of NWs. Then 200 SCCM of NH<sub>3</sub> flow is introduced without interruption of Ga vapour. The growth duration is fixed for one hour for all the samples. At the end the reactor is turned off to cool down to room temperature naturally.

The morphology and compositional variation of GaN NWs were studied using field emission scanning electron microscopy (FESEM) (Carl Zeiss - Sigma) equipped with energy dispersive X-ray analysis (EDX) (Oxford instruments). EDX has been recorded at 10 keV with the point resolution of around 10 nm. High resolution transmission electron microscope (HRTEM) (JEOL- 2010-200 kV) was carried out to examine the crystallinity of a single GaN nanowire. TEM samples were prepared by scratching GaN NWs from the substrate, dispersing them in ethanol, and casting a drop of the suspension on a Cu-grid coated with porous carbon thin film. Photoluminescence (PL) spectrum for the ensemble of NWs have been recorded by using the He-Cd laser of 325 nm (power – 30mW) as an excitation source

and the resulting luminescence signal has been analyzed through a monochromator (Horiba Jobin Yvon – 0.55 M) with a charge coupled device.

Photocatalytic experiments were performed in an apparatus specially designed for the photocatalytic reaction. The photocatalytic degradation of Methylene Blue (MB) was chosen to investigate the activity of GaN nanowires as it is one of the important industrial dyes. In a typical experiment, GaN NWs (Figure S1 - supporting information) on Si substrate (1 x 1 cm<sup>2</sup>) was suspended inside the 50 ml of aqueous solution containing 10 mg/L of MB dye. Prior to irradiation, the suspension was kept to attain adsorption-desorption equilibrium by aeration for 30 min in dark. The photocatalytic activity was investigated under UV and visible light irradiation using 125 W medium pressure mercury lamp emitting at 365 nm (110 μW cm<sup>-2</sup>, measured by Lutron UV light Meter) and 300W Tungsten Halogen lamp (8500 lumen), respectively. The distance between the light source and mouth of a glass bottle was 16 cm to reduce the heat radiation from the lamp. The reaction solution was kept under illumination for 240 min and 180 minutes for UV and visible light irradiations, respectively. At certain intervals of time, aliquots (1 mL) of the solution were taken out and the degradation of MB dye was determined by measuring the maximum absorbance at 554 nm on UV - Visible Spectrophotometer. The concentration of MB in the solution at various reaction times was determined using a calibration curve of absorbance against standard solutions (10 mM). In order to avoid the photosensitization effect, the whole reaction was carried out under the flow of noble gas (Ar) to carry away the degraded gas molecules out of the reaction chamber. The percentage of degradation of MB was calculated by the following equation (eqn (1)).

$$D = \frac{(A_0 - A_t)}{A_0} * 100 \text{ ----- (1)}$$

where,  $D$  is the percentage of degradation,  $A_0$  and  $A_t$  are initial absorption and absorption at time  $t$ , respectively. Photocatalytic degradation of organic compounds usually follows pseudo-first order kinetics model. The rate constant for the degradation of MB is calculated using the following Langmuir-Hishelwood kinetic equation.

$$\ln \frac{C_0}{C} = K_{app} t \text{ ----- (2)}$$

where,  $C_0$  is the initial concentration of the dye solution ( $\text{mol L}^{-1}$ ),  $C$  is the concentration of the dye solution at time  $t$  ( $\text{mol L}^{-1}$ ),  $k_{app}$  is the apparent rate constant ( $\text{min}^{-1}$ ). The rate constant for the degradation of MB was calculated from the slope of plot  $\ln(C_0/C)$  Vs irradiation time.

### Results and Discussion:

Figure 1 (a) shows the quasi aligned GaN NWs grown with the self-catalytic approach having the average diameter and length of  $\sim 160$  nm and  $10 \mu\text{m}$ , respectively. Fig 1(b) shows TEM image recorded on a single GaN NW that reveals the un-tapered straight NW. Inset of Fig. 1 (b) shows the selected area electron diffraction (SAED) pattern recorded on the body of a single NW. Figure 1(c) shows the HRTEM image of GaN NW which contains defects such as stacking faults and cubic inclusion. Besides wurtzite structure, the presence of cubic inclusions and stacking faults is also evidenced by the SAED pattern. Deep investigations on the HRTEM analysis are warranted to map the defect formation and propagation which is beyond the scope of this manuscript. EDX recorded on the ensembles of NWs shows (Figure 1(d)) almost equimolar atomic concentration of Ga and N.

Figure 2 (a) shows the Ni-nanodots after annealing a 5 nm thick Ni film coated Si substrate for 15 minutes at  $900^\circ\text{C}$  under vacuum. Figure 2 (b) shows the tilt-view FESEM image of high yield quasi-aligned Ni-catalyst assisted GaN NWs grown on Si(111) substrates. The average diameter and length of the NWs are  $\sim 120$  nm and  $10 \mu\text{m}$ ,

respectively. EDX recorded (Inset of Fig 2(b)) on the ensembles of GaN NWs shows almost equimolar Ga to N ratio in addition to the presence of other elements such as Ni and substrate impurities of Si and O. The presence of O from the elemental analysis has been attributed to the presence of strong native oxide of Si substrate. Figure 2(c) presents a detailed HRTEM examination on the interface between the NW and the catalyst droplet of a single GaN NW which indicates that the interface is abrupt and smooth. Figure 2(d) shows the NW is free of domain boundaries and cubic inclusion having a single-crystalline nature. SAED pattern (Inset of Fig. 2(d)) shows that the NW took the wurtzite structure and grew along [100].<sup>22</sup>

Figure 3(a) and (b) show the FESEM images of Au catalyst assisted GaN NWs. The average diameter and length of the NWs were 150 nm and 10  $\mu\text{m}$ , respectively. Figure 2(c) show the TEM image recorded on the single nanowire reveals the presence of Au catalyst on the top of the NW. SAED pattern recorded (Inset of the Fig. 2(c)) on the NW shows the hexagonal wurtzite crystal structure. Figure 2 (d) shows HRTEM recorded on the body of a single NW, which reveals that the NWs are free from defects such as cubic inclusion and having a single-crystalline nature. The NW diameter is apparently very homogeneous from top to bottom without any tapering effect. The structural quality of Au assisted GaN NWs and Ni assisted GaN NWs are very similar.

Room temperature photoluminescence (PL) spectrum has been recorded on the ensembles of GaN nanowires. Figure 4 (a), (b) and (c) shows the PL spectra for self-catalyst and catalyst assisted GaN NWs. In all the GaN NWs grown under various catalysts the band edge emission at 3.4 eV dominates the luminescence spectra, which reveal the good optical quality of the GaN NWs. For Ni-catalyst assisted GaN NWs (Fig. 4(c)), in addition to the band edge at 3.43 eV, the broad Donor Acceptor Pair recombination (DAP) emission is also observed at 3.28 eV. The shallow DAP has been attributed to defects such as  $\text{Si}_{\text{Ga}}$  and  $\text{O}_{\text{N}}$  as

both the defects are quite possible in our growth approach.<sup>23</sup> Si has high solubility in both Ni and Au, hence the NWs can have Si interstitials and/or  $\text{Si}_{\text{Ga}}$  type defects. Further, it has been widely reported that the catalytic grown GaN NWs on Si substrates can be unintentionally doped with Si. In addition with Si, O could also be incorporated into the growing NW from the complex native oxide layer of Si. The other source for  $\text{O}_2$  could be from the atmospheric transfer of samples for analysis. There are no other peaks are visible for Ni-catalyst assisted GaN NWs.

For Au-catalyst assisted GaN NWs (Fig. (4 (b))), the band edge is observed at 3.41 eV, slightly red shifted from Ni-catalyst assisted NWs. In addition to band edge emission, three other peaks were also clearly resolved from the Lorentzian curve fitting. The peak at 2.98 eV has been attributed to the DAP type peak, owing to defects such as  $\text{Si}_{\text{Ga}}$  and  $\text{O}_{\text{N}}$ .<sup>24</sup> The peak centered at 3.01 eV can be assigned as Blue luminescence (BL) band of GaN. BL band at room temperature can be attributed to the escape of holes from the acceptor to the valence band and/or the bound holes may non-radiatively recombine with free electrons in the conduction band. Generally the BL band is related to a shallow acceptor ( $\text{Si}_{\text{N}}$  or  $\text{C}_{\text{N}}$ ) and the origin of this BL band is still a topic of considerable debate in literature.<sup>25</sup> The Peak at 2.20 eV has been attributed to the Yellow Luminescence (YL) of GaN. In most of the unintentionally and intentionally doped n-type GaN samples grown by the various techniques available, the room-temperature PL spectrum contains YL band centering at 2.10–2.25 eV.

For self-catalytic assisted GaN NWs (Fig. 4(a)) the band edge emission is centered at 3.39 eV, which is 0.3 eV red shifted from Ni-catalyst assisted GaN NWs. In addition to the band edge emission, two additional peaks were also resolved. The BL band is centered at 3.02 eV and the intense YL band is observed at 2.1 eV. The YL band is split into two peaks and the intensity of YL band is very dominant and comparable with the band edge emission

of GaN. Here, the dominant defect related YL band has been attributed to the several defects such as  $V_{Ga}$ ,  $V_N$  and complex defects related that gives rise to emission at 2.1 eV.<sup>26</sup> It is also worth to note that both the self-catalytic and Au-catalytic assisted GaN NWs possesses considerable defect related emissions in the visible region, whereas Ni-catalyst assisted GaN NWs does not show any defect related emissions in the visible region including YL band owing to high optical quality of NWs. The energy level diagram for self-catalytic GaN NW with defect induced intermediate energy levels and degradation kinetics of dye molecule is illustrated in Figure 4 (d).

It is well-known that the dye industry has a problem of disposal of MB due to their high solubility in water. Traces of these dyes are harmful to human beings. It causes skin diseases and intestinal problems. In view of this, the photocatalytic activity of the prepared GaN NWs for the degradation of MB is demonstrated under UV and visible irradiation. This reaction is chosen because both the electron and hole end up participating in the production of OH radical, which degrades the MB and the extent of the reaction can be monitored through optical absorption. We have studied the photocatalytic dye degradation properties for Ni-catalyst assisted GaN NWs, Au-catalyst assisted GaN NWs and self-catalytic GaN NWs. In addition the results are compared with the MOCVD grown 2  $\mu\text{m}$  thick GaN epitaxial layers. Special care was paid to the evaporation loss during the illumination. Before the photocatalytic reaction, two separate tubes consisting of 1) GaN NWs immersed in MB solution was kept under dark conditions and 2) MB solution without GaN NWs was also kept at UV and Visible irradiation. The results show that MB colour remained unaffected in the presence of GaN NWs under dark conditions and further no photochemical reaction of the dye occur under UV and visible light in the absence of the GaN NWs. Therefore, both UV/Visible illumination and semiconductor catalysts (GaN NWs) are necessary for the efficient decolourization reaction to occur.

Figure 5(a) and (b) show the photocatalytic degradation properties of GaN NWs for MB under UV and visible light irradiation with different time durations. UV-Vis absorption spectra of degraded MB solution (10 ppm) using as-synthesized GaN NWs is given in the supporting information (Figure S2 and S3). From UV-Vis absorption the concentration of MB in the solution was plotted as a function of irradiation time using Beer–Lamberts Law, and the results of different GaN NWs are compared in Figure 5(c) and (d). The changes of normalized concentration ( $C/C_0$ ) of MB with irradiation were assumed to be proportional to the normalized maximum absorbance ( $A/A_0$ ).

The Ni-catalyst assisted NWs shows the maximum degradation of 93% under UV irradiation for the duration of 240 minutes and the results of other samples are quite comparable with the Ni-catalyst assisted NWs. However, epitaxial GaN layer grown by MOCVD shows considerable low degradation percentage (~65%). Here, the results of photocatalytic dye degradation for various GaN NWs cannot be directly compared, because the photocatalytic activity depends directly on surface area of the NWs. However, it is clear that GaN NWs shows better photocatalytic activity than their epitaxial counterpart. From the UV absorption spectra, the peak at 662 nm (Figure S2 and S3 - supporting information) almost disappeared gradually without any considerable shift of the peak position upon UV-light exposure with time elapse which indicates that a cleavage of the aromatic ring of the dye molecule.

Surprisingly, photodegradation activity of GaN NWs increases under visible light irradiation and the maximum degradation of 89% for the self-catalytic GaN NWs have been achieved within 180 minutes. It is very important to note that Ni-catalyst assisted NWs shows better performance for photocatalytic degradation under UV light. However, in case of visible light the trend reverses and the photocatalytic degradation of self-catalytic GaN NWs shows

better degradation activity. These results can be understood by correlating the photocatalytic dye degradation property with the optical transitions in PL spectra.

Generally, the organic waste degradation is due to the oxidation by the photo generated carriers. Electrons generated in semiconductors during light irradiation contribute to reductions whose potential positioned between the conduction and valence bands, and the band gap of GaN possesses all the possible redox potentials.<sup>27</sup> It is quite well known that holes are responsible for the oxidation and electrons for reduction.<sup>28</sup> We believe that the electrons from the energy levels of surface defects such as vacancies produce excessive electron-hole recombination process. PL spectrum of self-catalytic GaN NWs shows the band edge emission at 3.42 eV in addition with the broad BL and YL band at 3.01 eV and 2.2 eV owing to the defect induced transitions. The spectrum encompasses the most visible region of the solar spectrum including UV-optical band edge emission for self-catalytic and Au-catalytic NWs. The samples dominant with the visible emission undergoes efficient photocatalytic decay of dyes in short span of time. Under visible irradiation sample produces high density electron-hole pairs on the surface of NWs which promotes decay of dyes due to oxidation process as the energy level matches with the redox potential of GaN with the organic pollutants (Figure 4(d)). The samples with high defect concentration including high non-radiative defects as well as high shallow donor concentration have been reported to exhibit low photocatalytic activity.<sup>29</sup> In general, the non-radiative point defects include recombination of electron-hole pairs via thermally emitting any optical emissions. Those defects do not contribute photo decay process there by reducing the efficiency. The radiative type defects induced BL and YL bands in self-catalytic and Au-catalytic assisted NWs are optically active in the solar spectrum which commensurate the enhancement of degradation under the visible light.

It is also quite possible to compare the luminescence intensity for various GaN NWs samples and its corresponding photocatalytic dye degradation activity. Though the optical intensity is directly depends on the density of NWs, the defects related intensity can be well compared with its own band edge. From this perspective, self-catalytic GaN NWs shows that YL band emission is comparable with the band edge emission. The BL band and YL band emissions are in the visible region and band edge emission is at the UV range. Hence, the higher photocatalytic activity of self-catalytic GaN NWs under visible region could be well triggered from the radiative type defects. For Ni-catalyst assisted GaN NWs, there are no visible BL and YL bands present, which corroborates the lower photocatalytic degradation under visible region while it demonstrated the maximum degradation of 93% under UV irradiation as due to dominant band edge at 363 nm.

GaN nanowires also have favorable reuse performance, which has been demonstrated by five successive recycling tests for photocatalytic reduction of MB. As shown in Figure 6, the nanowires exhibit almost no deactivation during five cycles of photoactivity test for the reduction of MB under visible light irradiation. The decay conversion efficiency of MB is nearly constant for each run. Therefore, the GaN nanowires can perform as a stable visible light driven photocatalyst towards selective reduction of azo dye compounds such as MB at room temperature under ambient atmosphere.

**Conclusion:**

The photocatalytic activity of wafer level GaN NWs grown under catalytic and self-catalytic approach has been investigated for the degradation of emergent organic pollutant dye - MB under UV and visible light irradiation. The self-catalyst assisted GaN NWs exhibits the high photocatalytic decay of 89% under visible light while Ni-catalyst assisted GaN NWs

decays 93% under UV irradiation. The higher photocatalytic activity of Ni-catalyst assisted GaN NWs under UV irradiation has been attributed to the dominant band edge emission at UV region. The optically active radiative defects in the visible region are responsible for the enhanced photocatalytic activity of self-catalytic GaN NWs under visible light. The defect engineered visible emission actively participates in the photocatalytic decay of dyes under solar spectrum and the results well corroborates with the room temperature photoluminescence emissions.

**Acknowledgements:**

Author K.J thanks Department of Science and Technology (DST), Govt. of India for the financial assistances under the Nanomission project No. SR/NM/NS-77/2008. V.P acknowledges CSIR, India for the award of senior research fellowship.

**Figure Captions:**

Figure 1 (a) shows the tilted view FESEM image of self-catalytic GaN NWs (b) shows TEM image of GaN NWs. Inset of (b) shows SAED pattern recorded on the body of the NW, (c) HRTEM recorded on the single NW shows the defects such as cubic inclusion and (d) EDX recorded on the ensembles of self-catalytic GaN NWs.

Figure 2 (a) shows the Ni - nanodots after annealing the Ni-coated Si substrate for 15 minutes (b) shows the tilted view FESEM image of Ni-catalyst assisted GaN NWs, inset of (b) shows the EDX recorded on the ensembles of the self-catalytic GaN NWs, (c) shows the HRTEM recorded on the interface between the catalyst and body of the NW and (d) shows the HRTEM recorded on the body of a single GaN NW. Inset of the figure shows the SAED pattern of single GaN NW

Figure 3 (a) and (b) show the FESEM images of Au-catalyst assisted GaN NWs (c) shows the TEM image of single GaN NW and the corresponding SAED pattern is shown in the inset of (c) and (d) shows the HRTEM recorded on the body of a single GaN NW.

Figure 4 show the room temperature photoluminescence spectra recorded on the ensembles of (a) self-catalytic GaN NWs, (b) Au-catalyst assisted GaN NWs, (c) Ni-catalyst assisted GaN NWs and (d) illustration of energy level diagram for GaN NW with defect induced intermediate energy levels and degradation kinetics of MB molecule.

Figure 5 show the photocatalytic dye degradation properties of various GaN NWs and its corresponding efficiency under UV (a, b) and visible light irradiation (c, d).

Figure 6 shows the reusability of GaN nanowires under visible light irradiation (a) Ni-catalyst assisted NWs, (b) Au-catalyst assisted NWs and (c) self-catalytic NWs. It clearly shows that the dye degradation efficiency of the nanowires does not reduce even after the 5 cycles of usage.

**Figures:**

Figure 1:

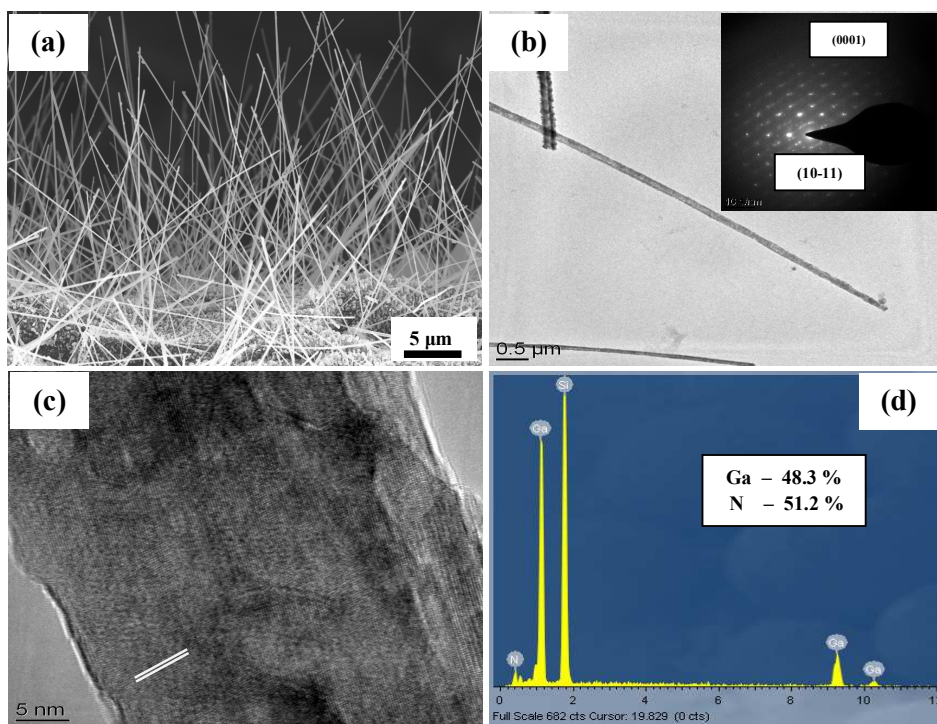


Figure 2:

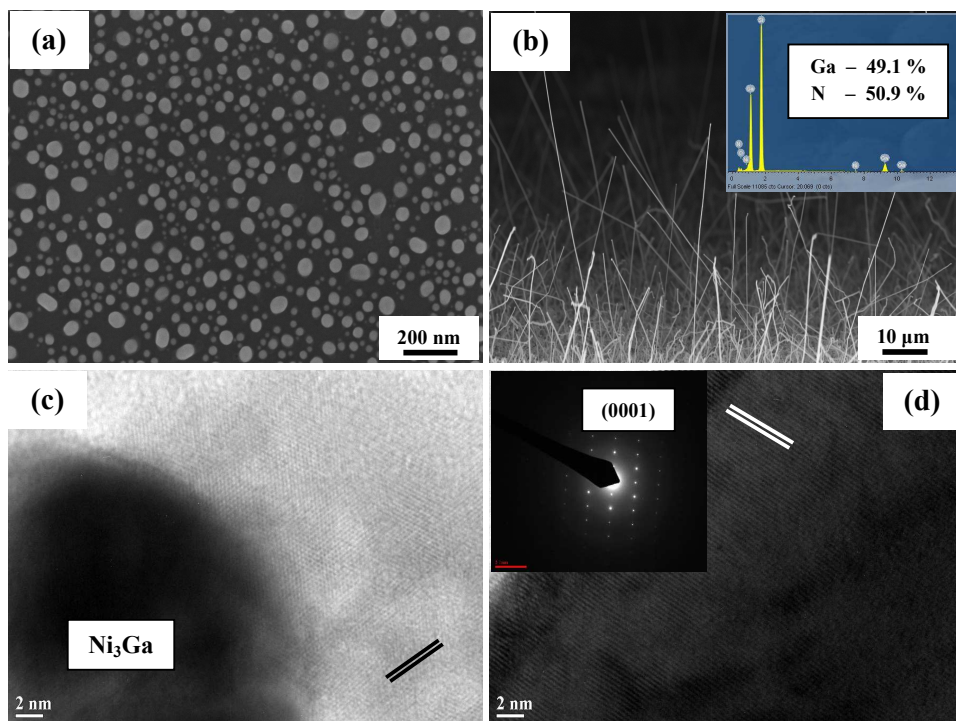


Figure 3:

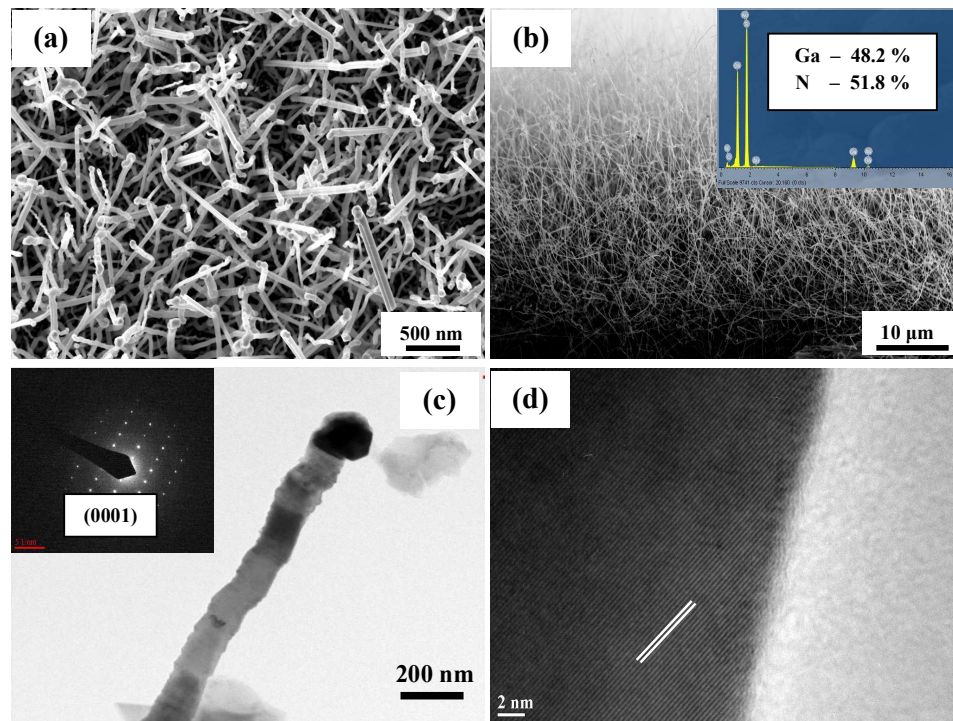


Figure 4:

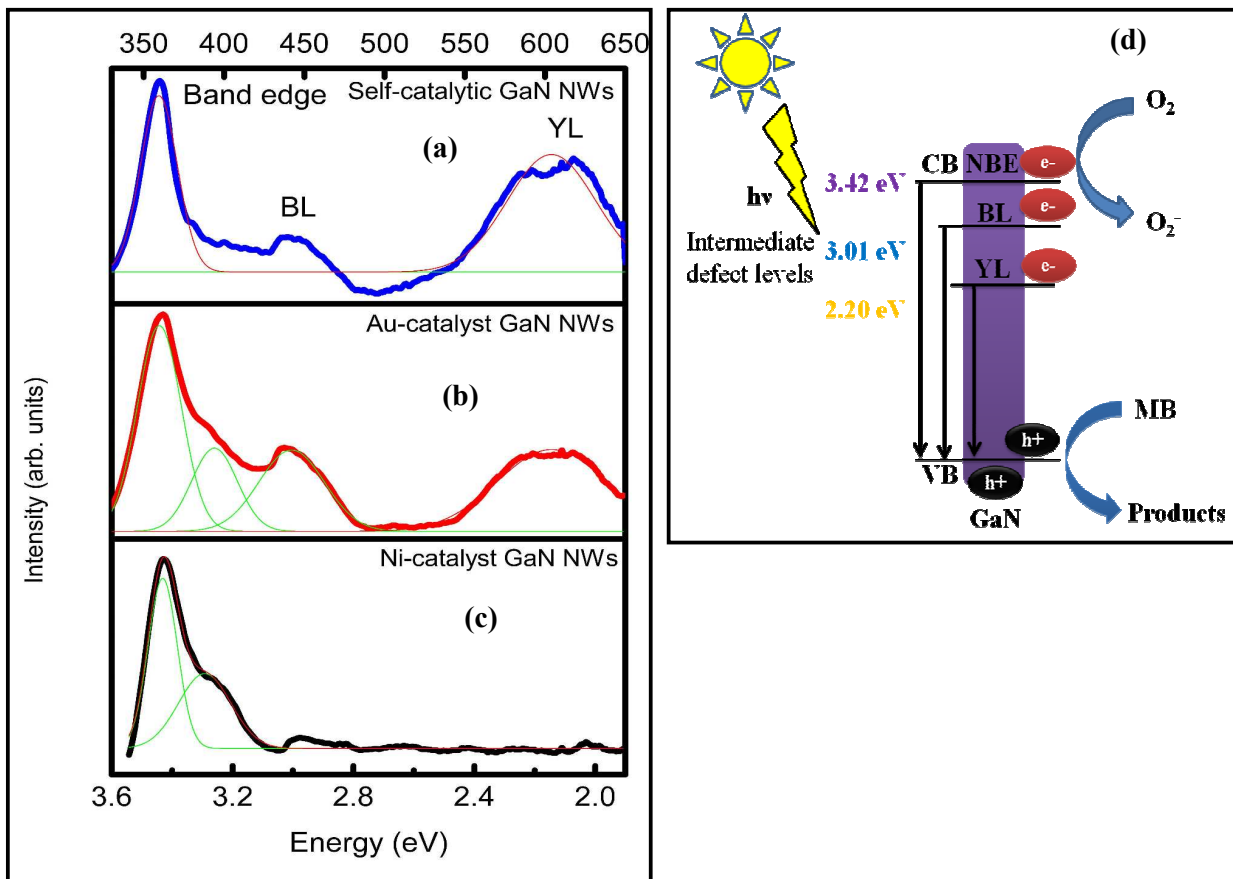
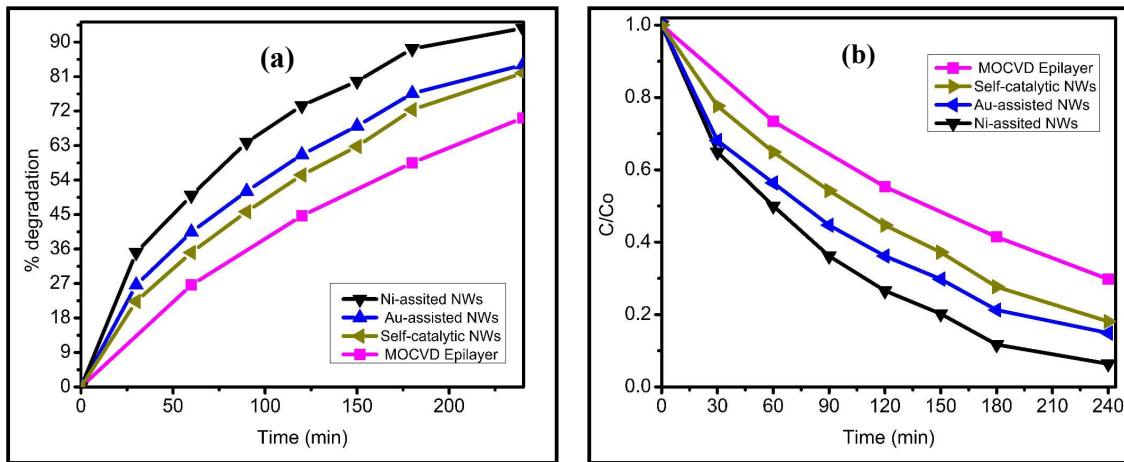


Figure 5:

UV light:



Visible light:

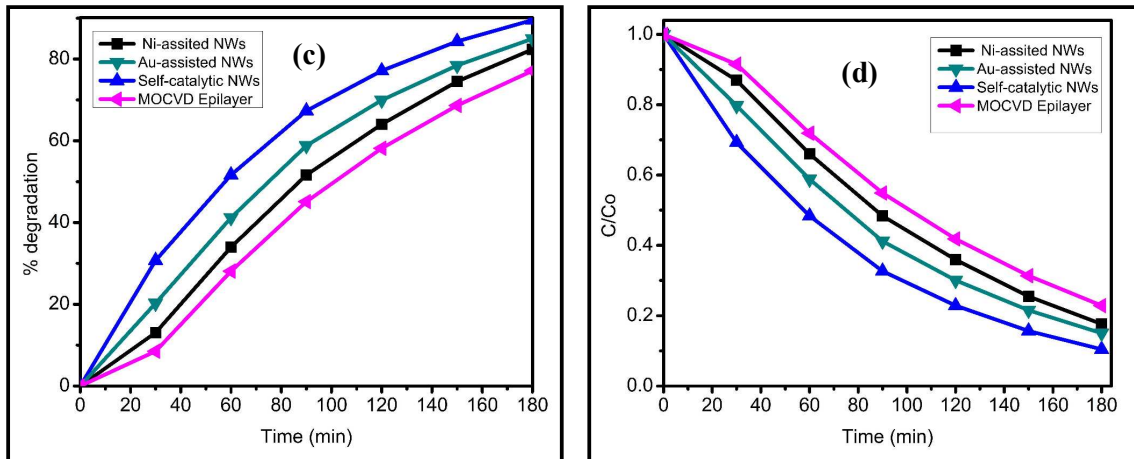
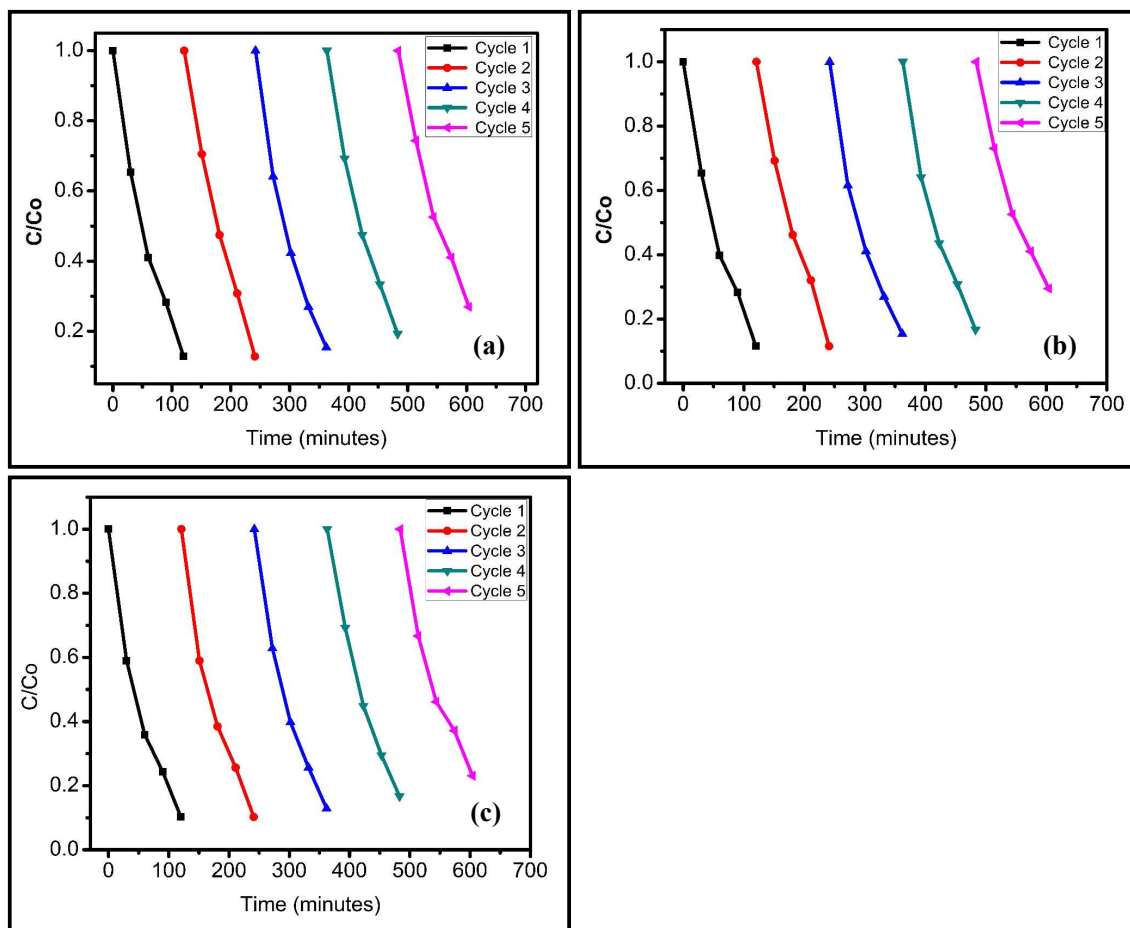


Figure 6:



## References

- <sup>1</sup> Z. Zou, J. Ye, K. Sayama and H. Arakawa, Direct splitting of water under visible light irradiation with an oxide semiconductor photocatalyst, *Nature*, **414**, 625-627, 2001.
- <sup>2</sup> A. Mills, R.H. Davies and D. Worsley, Water purification by semiconductor photocatalysis, *Chemical Society Reviews*, **22**, 417-425, 1993.
- <sup>3</sup> M. Grätzel, Dye-sensitized solar cells, *Journal of Photochemistry and Photobiology C: Photochemistry Reviews*, **4**, 145-153, 2003.
- <sup>4</sup> K. Vinodgopal, and P.V. Kamat, Enhanced Rates of Photocatalytic Degradation of an Azo Dye Using SnO<sub>2</sub>/TiO<sub>2</sub> Coupled Semiconductor Thin Films, *Environmental Science & Technology*, **29**, 841-845, 1995.
- <sup>5</sup> T. Wu, G. Liu, J. Zhao, H. Hidaka and N. Serpone, Photoassisted Degradation of Dye Pollutants. Self-Photosensitized Oxidative Transformation of Rhodamine B under Visible Light Irradiation in Aqueous TiO<sub>2</sub> Dispersions, *The Journal of Physical Chemistry B*, **102**, 5845-5851, 1998.
- <sup>6</sup> S. Chakrabarti and B.K. Dutta, Photocatalytic degradation of model textile dyes in wastewater using ZnO as semiconductor catalyst. *Journal of Hazardous Materials*, **112**, 269-278, 2004.
- <sup>7</sup> S. Sakthivel, B. Neppolian, M.V. Shankar, B. Arabindoo, M. Palanichamy, V. Murugesan, Solar photocatalytic degradation of azo dye: comparison of photocatalytic efficiency of ZnO and TiO<sub>2</sub>. *Solar Energy Materials and Solar Cells*, **77**, 65-82, 2003.
- <sup>8</sup> M. Shen, X. Zhang, K. Dai, H. Chen and T. Peng, Hierarchical PbMoO<sub>4</sub> microspheres: hydrothermal synthesis, formation mechanism and photocatalytic properties, *CrystEngComm*, **15**, 1146-1152, 2013.
- <sup>9</sup> K. Dai, Y. Yao, H. Liu, I. Mohamed, H. Chen, Enhancing the photocatalytic activity of lead molybdate by modifying with fullerene, *Journal of Molecular Catalysis A: Chemistry*, **374-375**, 111-117, 2013.
- <sup>10</sup> C. Liu, H. Chen, K. Dai, A. Xue, H. Chen, Q. Huang Synthesis, characterization, and its photocatalytic activity of double-walled carbon nanotubes-TiO<sub>2</sub> hybrid, *Materials Research Bulletin*, **48**, 1499-1505, 2013.
- <sup>11</sup> K. Dai, H. Chen, T. Peng, D. Ke, H. Yi, Photocatalytic degradation of methyl orange in aqueous suspension of mesoporous titania nanoparticles, *Chemosphere*, **69**, 1361-1367, 2007.
- <sup>12</sup> K. Dai, T. Peng, D. Ke and B. Wei, Photocatalytic hydrogen generation using a nanocomposite of multi-walled carbon nanotubes and TiO<sub>2</sub> nanoparticles under visible light irradiation, *Nanotechnology*, **20**, 125603, 2009.
- <sup>13</sup> K. Dai, X. Zhang, K. Fan, T. Peng, B. Wei, Hydrothermal synthesis of single-walled carbon nanotube-TiO<sub>2</sub> hybrid and its photocatalytic activity, *Applied Surface Science*, **270**, 238-244, 2013.
- <sup>14</sup> J. C. Johnson, H. J. Choi, K. P. Knutsen, R. D. Schaller, P. Yang, and R. J. Saykally, Single gallium nitride nanowire lasers. *Nature Materials*, **1(2)**, 106-110, 2002.
- <sup>15</sup> P. D. Ye, B. Yang, K. K. Ng, J. Bude, G. D. Wilk, S. Halder and J. C. M. Hwang, GaN metal-oxide-semiconductor high-electron-mobility-transistor with atomic layer deposited Al<sub>2</sub>O<sub>3</sub> as gate dielectric, *Applied Physics Letters*, **86**, 063501, 2005.

- 
- <sup>16</sup> C.J. Barrelet, A.B. Greytak, and C.M. Lieber, Nanowire Photonic Circuit Elements. *Nano Letters*, **4**(10), 1981-1985, 2004.
- <sup>17</sup> J.L. Yang, S.J. An, W.I. Park, G.C. Yi and W. Choi, Photocatalysis Using ZnO Thin Films and Nanoneedles Grown by Metal-Organic Chemical Vapor Deposition. *Advanced Materials*, **16**(18), 1661-1664, 2004.
- <sup>18</sup> Y.S. Kim, I. S. Hwang, S. J. Kim, C.Y. Lee, J. H. Lee, CuO nanowire gas sensors for air quality control in automotive cabin. *Sensors and Actuators B: Chemical*, **135**, 298-303, 2008.
- <sup>19</sup> V. Purushothaman, and K. Jeganathan, Structural Evolution and Growth Mechanism of Self-Assembled Wurtzite Gallium Nitride (GaN) Nanostructures by Chemical Vapor Deposition. *The Journal of Physical Chemistry C*, **117**, 7348-7357, 2013.
- <sup>20</sup> V. Purushothaman, V. Ramakrishnan and K. Jeganathan, Whiskered GaN nanowires by self-induced VLS approach using chemical vapor deposition. *CrystEngComm*, **14**, 8390-8395, 2012.
- <sup>21</sup> V. Purushothaman, V. Ramakrishnan and K. Jeganathan, Interplay of VLS and VS growth mechanism for GaN nanowires by a self-catalytic Approach, *RSC Advances*, **2**, 4802, 2012.
- <sup>22</sup> X. Duan, and C.M. Lieber, Laser-Assisted Catalytic Growth of Single Crystal GaN Nanowires. *Journal of the American Chemical Society*, **122**, 188-189, 1999.
- <sup>23</sup> A. Soudi, E. H. Khan, J. T. Dickinson and Y. Gu, Observation of Unintentionally Incorporated Nitrogen-Related Complexes in ZnO and GaN Nanowires. *Nano Letters*, **9**(5), 1844-1849, 2009.
- <sup>24</sup> J. Liu, X. M. Meng, Y. Jiang, C. S. Lee, I. Bello and S. T. Lee, Gallium nitride nanowires doped with silicon. *Applied Physics Letters*, **83**, 4241-4243, 2003.
- <sup>25</sup> M.A. Reshchikov and H. Morkoç, Luminescence properties of defects in GaN. *Journal of Applied Physics*, **97**, 061301, 2005.
- <sup>26</sup> Thillozen, N., K. Sebal, H. Hardtdegen, R. Meijers, R. Calarco, S. Montanari, N. Kaluza, J. Gutowski, and H. Lüth, The State of Strain in Single GaN Nanocolumns As Derived from Micro-Photoluminescence Measurements. *Nano Letters*, **6**, 704-708, 2006.
- <sup>27</sup> H.S. Jung, Y. J. Hong, Y. Li, J. Cho, Y. J. Kim and G. C. Yi, Photocatalysis Using GaN Nanowires, *ACS Nano*, **2**, 637-642, 2008.
- <sup>28</sup> B. Liu, A. Khare, and E.S. Aydil, TiO<sub>2</sub>-B/Anatase Core-Shell Heterojunction Nanowires for Photocatalysis, *ACS Applied Materials & Interfaces*, **3**, 4444-4450, 2011.
- <sup>29</sup> F. Liu, Y. H. Leung, A. B. Djurišić, A. M. C. Ng, and W. K. Chan, Native Defects in ZnO: Effect on Dye Adsorption and Photocatalytic Degradation, *The Journal of Physical Chemistry C*, **117**, 12218-12228, 2013.